RSC Advances

ROYAL SOCIETY OF CHEMISTRY

www.rsc.org/advances

Quick synthesis, functionalization and properties of uniform, luminescent $LuPO_4$-based nanoparticles.

Ana I. Becerro and Manuel Ocaña*

Instituto de Ciencia de Materiales de Sevilla (CSIC-University of Seville).
c/ Américo Vespucio, 49. 41092 Seville (Spain).

* Corresponding author. E-mail address: anieto@icmse.csic.es. Tel no: +34 95448945. Fax no: 954460165

Abstract

The aim of this study was to find a surfactant-free method for the synthesis of uniform Eu:$LuPO_4$ nanophosphors which are able to form stable colloidal suspensions in aqueous media. Uniform, ovoid Eu-doped $LuPO_4$ fluorescent nanoparticles were obtained after aging for 30 minutes at 180ºC a butylene glycol solution containing, exclusively, lutetium acetate, europium acetate and H_3PO_4. XRD and digital diffraction patterns of HRTEM images suggested that the particles were single crystals in nature with the *c*-axis of the unit cell parallel to the long particle axis. The luminescence study revealed that the optimum doping level was 5 molar %. The latter particles (85 nm x 40 nm dimensions) were functionalized with polyacrylic acid and their colloidal stability in two different biological buffers was demonstrated to persist for at least 15 days.

1. Introduction

Lanthanide-doped nanomaterials form an important class of luminescent materials which are suitable for both down- and up conversion processes.[1] Their narrow emission bands as well as the long luminescence decay times in the range of the milliseconds make these materials interesting for applications not only in the optoelectronic field[2,3] but also in biotechnology.[4,5] Among the large number of lanthanide compounds, rare earth orthophosphates ($REPO_4$) represent an important class of materials that can be used in a large variety of applications as luminescent or laser materials and also in medicine.

For many of these applications it is highly desirable to have uniform nanoparticles with controlled size and shape, as well as good dispersion.[2,5] Many research groups have reported, in the last decade, on the doping of YPO_4, $LaPO_4$, $CePO_4$, and $GdPO_4$ nanoparticles with ions of the *f*-elements for optoelectronic as well as biotechnological applications.[6,7,8,9,10,11,12,13] However, very few reports have been found in the literature which describe the synthesis of $LuPO_4$ particles. Gao et al.[14] reported the synthesis of uniform $LuPO_4$ hollow spheres using a two-step urea-based process which rendered particles with a diameter of around 300 nm, well above the size of nanometer-scale materials. To the best of our knowledge, only two papers have reported the synthesis of monodisperse, nanometer-size $LuPO_4$ particles.[15,16] In both cases a rather tedious synthesis method was used based on the use of several organic additives. The inconvenience of these additives is that they remain attached to the surface of the particles making them hydrophobic. A challenge for bioanalytical or therapeutic applications of this material is to find new synthesis routes to produce nanoparticles that can be dispersed in aqueous media to form stable colloidal solutions.

In the present study, we report a quick and really simple method to synthesize uniform Eu- doped $LuPO_4$ nanometer size particles, with optimized luminescent properties. The method is based on a homogeneous precipitation process in a solution containing, exclusively, Ln^{3+} (Lu^{3+}, Eu^{3+}) acetates and H_3PO_4. We have investigated the influence of the precursor nature and concentration as well as the type of solvent on the morphology of the precipitated particles. The particles have eventually been functionalized with polyacrylic acid (PAA) to demonstrate that they can be easily surface-modified to provide anchor sites for functional ligands.[17] Finally, the colloidal

stability of the PAA-functionalized particles has been analyzed in different biological buffers (MES and PBS).

2. Experimental section

2.1. Synthesis of samples

The $LuPO_4$ nanoparticles were obtained according to the following method: Lutetium acetate hydrate ($Lu(CH_3COO)_3 \cdot xH_2O$, Sigma Aldrich, 99.9%) was dissolved, with magnetic stirring, in 10 mL of butylene glycol (BG, Fluka, 99.5%) to obtain a 0.025 M solution. The solution was admixed with H_3PO_4 (0.1 M) and magnetically stirred for 5 minutes at room temperature to favor homogenization. The final solution was aged for 30 minutes in tightly closed test tubes using an oven preheated at 180 ºC. The resulting dispersion was cooled down to room temperature, centrifuged to remove the supernatants and washed, twice with ethanol and once with double distilled water. For some analyses, the powder was dried at room temperature. Other values of aging time (from 4 to 30 minutes) as well as different Lu and PO_4 sources were used to analyze their effect on the particles characteristics. Such sources were $Lu(NO_3)_3$ (Sigma Aldrich, 99.99%) and 1-Butyl-3-methylimidazolium phosphate ([BMIM][PO_4] 99% Strem Chemicals), for Lu and PO4, respectively. We also used solvents other than BG to analyze their effect on the particles morphology. The solvents used were ethylene glycol (EG, Sigma Aldrich, 99.99%) and glycerol (Gly, Sigma Aldrich > 99.5%).

The Eu^{3+}-doped particles were synthesized following the same procedure and using Eu^{3+} acetate hydrate ($Eu(CH_3COO)_3 \cdot xH_2O$, Sigma Aldrich, 99.9%) in variable amounts. The lanthanide ions (Lu + Eu) concentration was kept constant (0.025 $mol \cdot dm^{-3}$) in all experiments, whereas the Eu/(Lu + Eu) molar ratio was varied from 0.5% to 15% in order to investigate the effect of this parameter on the morphological and luminescent properties of the precipitated particles.

2.2. Functionalization of the particles with polyacrylic acid (PAA)

The procedure for the functionalization of the Eu^{3+}-doped $LuPO_4$ nanoparticles was as follows: PAA (average Mw ~ 1800, Aldrich) was added to solutions with adjusted pH (10) containing 1 mg /mL of the Eu^{3+}:$LuPO_4$ nanoparticles (PAA/Eu^{3+}:$LuPO_4$ weigh

ratio = 2). The obtained dispersion was magnetically stirred for 1 hour at room temperature. The so functionalized nanoparticles were washed several times with milliQ water by centrifugation and finally dispersed in milliQ water.

2.3. Characterization techniques

The shape and size of the particles was examined by both *transmission electron microscopy* (*TEM*, Philips 200CM) and *scanning electron microscopy* (*SEM-FEG* Hitachi S4800). Particle size distributions were obtained from the micrographs by counting several hundreds of particles, using the free software *ImageJ*. Additional information on the size and colloidal stability of the particles in aqueous suspension (0.5 $mg \cdot mL^{-1}$ of solid) was obtained from *Dynamic Light Scattering* (*DLS*) measurements. The experiments were carried out using a Malvern Zetasizer Nano-ZS90 equipment, which was used as well to measure the Zeta potential of the suspensions.

The crystalline structure of the prepared particles was assessed by *X-ray diffraction (XRD)* using a Panalytical, X´ Pert Pro diffractometer (CuKα) with an X-Celerator detector over an angular range of $10º < 2\theta < 120º$, 2θ step width of 0.02º, and 10 s counting time. The crystallite size was calculated using the Scherrer formula from the full width at half maximum of several single reflections. To gain additional information about the crystalline features of the synthesized nanoparticles, they were also characterized by *high-resolution transmission electron microscopy (HRTEM)* using a FEGTEM Tecnai 20 instrument. The TEM images were acquired with an Ultrascan X100 camera from Gatan. Digital diffraction patterns were also calculated by Fourier Transform of such HRTEM images using the Gatan Digital Micrograph software.

The incorporation of Eu^{3+} into the $LuPO_4$ structure was proved by calculation of unit cell parameters of the undoped and the Eu^{3+}-doped particles. For this purpose, the corresponding XRD patterns were analyzed using the Rietveld method with the TOPAS software (TOPAS version 4.2, Bruker AXS, 2009). Starting crystallographic parameters were taken from those reported for tetragonal $LuPO_4$.[18] Nominal Eu^{3+} contents were added to the structure. Refined parameters were: scale factor, zero error, background coefficients, unit cell parameters and atomic coordinates and atomic displacement factors of the lanthanide atoms.

The *infrared spectra* of the powders, diluted in KBr pellets, were recorded in a Jasco FT-IR-6200 Fourier transform spectrometer.

Thermogravimetric analyses were performed in air at a heating rate of 10ºC·min^{-1} using a Q600 TA instrument.

The *excitation and emission spectra* of the Eu^{3+}-doped $LuPO_4$ particles, dispersed in water (2.5 mg·mL^{-1}), were measured in a Horiba Jobin Yvon spectrofluorimeter (Fluorolog3). The emission spectra were transformed to the CIE color coordinates system using a 2º observer.

The *colloidal stability* of Eu:$LuPO_4$ nanoparticles (0.5 mg·mL^{-1} of solid) suspended in different media (milliQ water, 50 mM MES solutions (2-(N-morpholino) ethanesulfonic acid, Sigma, 99%) at pH 6.5, and in 50 mM PBS (Phosphate Buffered Saline) solution at pH 7.2) was monitored by analyzing the evolution of the hydrodynamic diameter, obtained from DLS measurements, with aging time.

3. Results and discussion

3.1. Morphology and crystal structure

The optimum experimental conditions for the synthesis of luminescent $LuPO_4$-based particles were established on the undoped material. It was found that the aging at 180ºC for 30 minutes of a butylene glycol (BG) solution containing Lutetium acetate (0.025 M) and H_3PO_4 (0.1 M) led to uniform ovoid-like nanoparticles (Figure 1, top). The particle size (Figure 1, bottom), obtained from different TEM micrographs by counting about a hundred of particles, was 130 (s.d. 19) nm for the long axis length and 62 (s.d. 9) nm for the short axis length. Although the SEM and TEM micrographs shown in Figure 1 suggested that the particles were uniform and non-aggregated, this aspect was further confirmed by dynamic light scattering (DLS) measurements conducted on an aqueous suspension of the particles. The Zeta potential measured at the original pH (pH= 4) was very close to the isoelectric point. For this reason, we increased the pH of the suspension to 10.3, obtaining a Zeta potential value of -44(10) mV and a hydrodynamic diameter of 140 nm. These data confirm the absence of particles aggregation.

Figure 2 shows the XRD pattern of the product shown in Figure 1. All the reflections could be readily indexed to the tetragonal $LuPO_4$ phase in $I4_1/amd$ space group (ICDD 00-043-0003, PDF4+, 2013). The SEM and TEM images shown in Figure 1 allow observing only two dimensions of the particles: their length and their width. If the particles were flat, their third dimension would be very small and they would lay with their flat faces parallel to the sample holder. This fact would notably increase the intensity of certain reflections in the XRD pattern of the sample due to the preferred orientation effect, as observed for flat particles by other authors.[19] Given that all the reflections in the XRD pattern match those of the standard PDF (LuPO4, 00-043-0003), it can be concluded that the sample is free from preferred orientation effects and that the $LuPO_4$ particles show very likely an ovoid morphology.

The crystalline domain sizes of the particles, calculated using the Scherrer formula on the (200) reflection were of ~70 nm and ~120 nm on the (101) reflection. These values are very close to the particles dimensions inferred from the TEM micrographs and suggest that the particles could be single crystals in nature. In fact, a close inspection of the particles by means of HRTEM (Figure 3a), allows observing lattice fringes going all along the particle long axis and regularly spaced at 3.5 Å from each other (see intensity profile in the inset of Figure 3a). This distance corresponds to the (002) interplanar distance of the tetragonal $LuPO_4$ phase and indicates that the *a* axis of the unit cell is parallel to the short axis of the particle. In order to learn about the orientation of the other two axis of the unit cell, we have calculated the digital diffraction pattern (DDP) from the area selected in Figure 3b and magnified in Figure 3c. The DDP (shown as inset in Figure 3c) shows a set of spots that correspond to the [010] zone axis of tetragonal $LuPO_4$. The spots assigned to the (200) planes of such phase are aligned perpendicular to the long axis of the particles while the ones assigned to the (101) planes are forming 48º with the former. These data confirm that the *a*-axis of the unit cell is parallel to the short axis of the particle and indicate that the *c*-axis is parallel to the long axis of the particle.

3.2. Influence of the synthesis conditions on the morphology of the precipitated particles.

The set of experimental conditions used above for the synthesis of $LuPO_4$ nanoparticles (lutetium acetate and H_3PO_4 as Lu^{3+} and phosphate source, respectively, at 0.025M and 0.1 M concentrations, respectively, BG as polyol, and 180 ºC aging temperature) is essential to obtain uniform nano-particles. The variation of either the Lu^{3+} or phosphate source or their concentrations, or the polyol nature led either to bigger elongated particles, to irregular particles, or to highly aggregated nanoparticles, as observe in Figure S1 and detailed below.

As observed in Figure S1a, an important change in morphology (from uniform, dispersed ovoid particles to aggregated nanorods) was observed when Lutetium acetate was replaced by Lutetium acetylacetonate, which indicates a strong influence of the Lu^{3+} precursor on the morphological characteristics of the product, in agreement with the literature on particle synthesis in polyol medium.[20] On the other hand, the decrease of the Lu^{3+} concentration from 0.025 M to 0.010 M resulted in an increase of particle size (~350 nm x ~200 nm, Fig. S1b). This result can be understood in terms of the classical theory of solution nucleation and particle growth.[21] As the Lu^{3+} concentration decreases, the precipitation reaction is expected to become slower thus decreasing the number of nuclei which further grow to a higher size. Figure S2 is a plot of the particle length *vs*. Lu^{3+} concentration showing an exponential decay of the size as the Lu^{3+} concentration increases, as expected from the afore mentioned theory of nucleation and growth. The effect of the phosphate source was analyzed using NaH_2PO_4 and $NH_4H_2PO_4$ as alternative $[PO_4]^{-3}$ precursors. However, both compounds were insoluble in BG in the concentration required for comparison with H_3PO_4 (0.1 M). We used alternatively the ionic liquid ([BMIM]PO_4). Figure S1c shows the product obtained after changing the phosphate source to the ionic liquid and keeping the rest of experimental conditions unchanged. It consists, essentially, of tiny aggregated particles whose formation could be due to the possible adsorption of the BMIM cations on the $LuPO_4$ nuclei, thus limiting their growth. The concentration of H_3PO_4 had also a strong influence on the particle size. The decrease of the concentration to 0.05 M resulted in the formation of highly aggregated nanoparticles (Figure S1d). The significant change in particle morphology and size with decreasing H_3PO_4 concentration indicates a decrease of the precipitation rate, probably as a consequence of the decrease in the amount of phosphate anions available for precipitation. A similar effect was observed in the synthesis of $GdPO_4$ particles.[12]

Finally, the nature of the solvent was also found to be a critical factor for the formation of uniform particles since the use of glycerol (Gly) or ethylene glycol (EG) instead of BG, led to strongly aggregated, ill-defined nanoparticles (Figure S1e and S1f). These morphological differences could be assigned to the different values of viscosity and dielectric constant of the solvents, which may affect the diffusion processes required for nucleation and particle growth.

In summary, it can be concluded that the use of a solution of Lutetium acetate and H_3PO_4 in BG allows obtaining ovoid particles whose size can be tuned by changing the Lu^{3+} or the $(PO_4)^{3-}$ concentration in the precursor solution.

3.3. Formation mechanism of the $LuPO_4$ nanoparticles

To elucidate the mechanism for the formation of the $LuPO_4$ nanoparticles shown in Figure 1, time-dependent experiments (4 minutes, 10 minutes and 30 minutes) were carried out in the appropriate synthesis conditions (lutetium acetate and H_3PO_4 solution in BG, 0.025M and 0.1 M, respectively, aged at 180 ºC). TEM images of the corresponding intermediates are shown in Figure 4 along with the XRD pattern of each reaction product. After 4 minutes the TEM images showed an ill-defined precipitate with a certain degree of long range organization, as revealed by the three broad features observed in the corresponding XRD pattern. Precipitation of small ovoid particles was only observed after 10 minutes aging, which coexisted with the ill-defined precipitate. These new particles gave rise to sharp reflections in the XRD pattern, corresponding to tetragonal $LuPO_4$, which stand above the broad features characteristic of the first precipitate. Finally, after aging the solution for 30 minutes, the reaction product consisted, exclusively, of $LuPO_4$ nanoparticles, while the corresponding XRD pattern only showed the reflections characteristic of tetragonal $LuPO_4$.

The formation of a precipitate in the first stages of the reaction seemed to indicate that the formation of the final particles would proceed through an aggregation process. However, the HRTEM and DDP study presented above suggests that the mechanism for the formation of the nanoparticles implied dissolution of the gel-like precipitate and recrystallization to form the $LuPO_4$ nanoparticles. A similar behavior was observed for the formation of Fe_2O_3 particles.[22]

3.4. Synthesis and characterization of Eu^{3+}-doped $LuPO_4$ nanoparticles.

We have used Eu^{3+} doping, as a proof on concept, to analyze the luminescent properties of the resultant $LuPO_4$ phosphors. Four different compositions (2.5%, 5%, 10% and 15% Eu^{3+} in $LuPO_4$) were synthesized using the method reported above for the undoped material, and adding the corresponding amount of europium acetate in each case. It was found that the shape of the undoped particles was reproduced for the doped samples for doping levels up to 10% (Figure 5), although a significant decrease in particle size was observed with increasing the Eu^{3+} content (Table 1). At Eu^{3+} contents of 15%, the particles lost their original form and exhibited a high degree of aggregation (Figure S3). The latter composition was, therefore, not included in the luminescence study.

To confirm the presence of Eu^{3+} in the $LuPO_4$ crystal structure, the XRD patterns of the $LuPO_4$ particles doped with different Eu^{3+} contents (Figure S4) were analyzed by the Rietveld method to obtain the corresponding unit cell volumes. The values obtained have been plotted in Figure 6, where a linear increase of the volume can be observed with increasing Eu^{3+} content, in agreement with the bigger ionic radius of Eu^{3+} compared with that of Lu^{3+}.[23] This behavior satisfies Vegard´s law[24] and indicates that Eu^{3+} is replacing Lu^{3+} in the crystallographic sites of the $LuPO_4$ structure.

3.5. Study of the luminescence properties of the Eu^{3+}-doped $LuPO_4$ nanoparticles

The excitation spectra of the Eu^{3+}-doped $LuPO_4$ nanoparticles were recorded by monitoring the emission of the characteristic $^5D_0$-$^7F_1$ transition of Eu^{3+} at 593 nm. Figure 7 (top) shows the excitation spectrum corresponding to the 5% Eu^{3+}-doped sample. The rest of compositions showed very similar excitation spectra to this one. They all exhibited a set of sharp and well defined excitation bands, the most intense at 395 nm, which correspond to the *f-f* electronic transitions characteristic of the Eu^{3+} ions[25] and that have been assigned in the Figure. The high intensity band at $\lambda < 270$nm, partially observed in the spectrum, is known as Eu-O charge transfer band and it is due to the electron transfer from the fully occupied $2p^6$ orbital of the O^{2-} anion and the partially occupied 4f orbitals of Eu^{3+}.[26]

The emission spectra of the Eu^{3+}-doped $LuPO_4$ nanoparticles (molar % Eu^{3+} from 2.5% to 10%) recorded after excitation at 395 nm, are shown in Figure 7 (bottom). The observed emission bands correspond to the well-known $^5D_0$-^7F_J (J= 0, 1, 2, 3, 4) transitions of Eu^{3+}. The $^5D_0$-$^7F_1$ transition is due to the magnetic dipole (MD) transition of Eu^{3+} ions and it is independent of the symmetry of the Eu^{3+} site. However, the $^5D_0$-$^7F_2$ transition is a forced electric dipole (ED) transition, hypersensitive to the site symmetry of the Eu^{3+} ions.[1] The intensity of both emission bands is very similar (ratio of the integral areas MD/ED = 1.04), as observed also in Eu-doped $LaPO_4$ particles.[20] This result indicates that the Eu^{3+} ions are located at a site without inversion center,[27] in good agreement with the tetragonal *I4₁/amd* structure of $LuPO_4$, which locates the Lu atom at a *4a* site with D_{2d} point group symmetry.[18]

Although the emission spectra of all compositions were very similar to each other from a qualitative point of view, their absolute intensities varied significantly with increasing Eu^{3+} content. Figure 8 shows the integrated intensity of the emission spectrum obtained for each composition as a function of the Eu^{3+} content. The emission intensity increased linearly with increasing Eu^{3+} content, reaching a maximum at the $LuPO_4$:5% Eu^{3+} composition. The observed increase in luminescence intensity is clearly due to the progressive increase of emission centers as the doping concentration increases. After reaching a maximum, the luminescence intensity decreases with increasing the Eu^{3+} doping level. This fact, known as concentration quenching effect, is due to the energy transfer between adjacent luminescent centers and becomes significant when the Eu-Eu distance decreases as a result of the increase in doping level.[1]

The colloidal suspensions of the Eu^{3+}-doped $LuPO_4$ nanoparticles dispersed in water emit a strong red-orange luminescence under UV radiation with CIE coordinates (x=0.63, x= 0.37) at any Eu^{3+} content (Figure 8, inset).

3.6. Functionalization and colloidal stability of Eu^{3+}-doped $LuPO_4$ nanoparticles

The optimum Eu^{3+}-doping composition found in the luminescence analysis was further used to test the functionalization capacity of the particles. Polyacrylic acid (PAA) was used as the functionalizing molecule (see the followed procedure in the Experimental section) due to its highly hydrophilic nature, which is appropriate for applications in the

biotechnology field.[28] The success of the functionalization process was proved by FTIR spectroscopy. The FTIR spectra of the particles, before and after the functionalization process, are shown in Figure 9 (top), together with the FTIR spectrum of pure PAA. The spectrum of the nude particles consisted of a group of bands at < 1200 cm^{-1} corresponding to the stretching and bending vibrations of the phosphate group. The bands at 3420 cm^{-1} and 1635 cm^{-1} are due to adsorbed water on the particles surface.[14] The FTIR spectrum of the PAA-treated particles exhibited, in addition to the bands found in the spectrum of the nude particles, some extra signals in the 1800-1350 cm^{-1} region that correspond to the stretching vibrations of the carboxylate anion in the PAA polymer. This finding confirmed the incorporation of the polymer onto the surface of the nanoparticles, as concluded for other lanthanide-based particles.[29] The Zeta potential of the particles before and after functionalization was also a measure of the success of the process. Thus, while a value of 0.3 mV was registered in the nude particles at pH= 4, a charge reversal (Zeta potential = -38.5 mV) was observed for the treated particles at the same pH. Finally, the amount of PAA species attached to the nanoparticles surface was quantified by thermogravimetric analyses (TGA). The TGA curve obtained for the PAA-functionalized Eu^{3+}:$LuPO_4$ nanoparticles is shown in Figure 9 (bottom), along with the curve corresponding to the particles before functionalization. While the latter consists of a mass loss due to the release of water (~ 11% of the total mass) in the temperature range 20ºC - 300ºC, the TGA curve of the PAA functionalized Eu^{3+}:$LuPO_4$ nanoparticles exhibited an additional weight loss (from 300º up to 700ºC) that can be associated to the decomposition of the adsorbed PAA and represents ~ 4% of the total mass.

Finally, the colloidal stability of the PAA-functionalized Eu^{3+}:$LuPO_4$ particles was checked in two different biological media: MES (at pH=6.5) and PBS (at pH= 7.2) (see details in the Experimental section). The average hydrodynamic diameter of the nanoparticles remained unaltered (~ 90 nm) during at least 15 days of aging in both media (Figure 10), which indicated an excellent colloidal stability of the particles and their suitability for applications in biotechnology.

4. Concluding remarks

Uniform, ovoid Eu^{3+}-doped lutetium orthophosphate nanoparticles (85 nm x 40 nm) have been synthesized using a quick, simple, and green method based on the homogeneous precipitation of ions in a butylene glycol solution containing, exclusively, Lu^{3+} and Eu^{3+} acetates (0.025 M) and H_3PO_4 (0.1 M) aged at 180ºC. The nanoparticles consisted of single crystals of tetragonal Eu:$LuPO_4$ and DLS measurements revealed that the particles were well dispersed in aqueous solution. The 5%Eu-doped $LuPO_4$ nanoparticles, were successfully functionalized with polyacrylic acid and showed a very high colloidal stability in two different biological buffers (MES, pH6.5 and PBS, pH= 7.2). These properties make the PAA-functionalized Eu:$LuPO_4$ nanoparticles good candidates as optical labels for in-vitro applications. Also their uniformity and luminescence characteristics indicate that the Eu:$LuPO_4$ nanoparticles are excellent materials for laser applications.

Acknowledgements

Supported by MEC (Project. MAT2012-34919), Junta de Andalucía (JA FQM 06090) and CSIC (201460E005). Olga Montes is gratefully ackowledged for help with *Tecnai 20* instrument.

Electronic supplementary information available:

- SEM micrographs of $LuPO_4$ samples prepared changing one of the experimental conditions described in Figure 1 of the paper and keeping the rest constant (Figure S1).

- Plot of average particle length versus Lutetium acetate concentration. The rest of synthesis conditions are identical to those given in Figure 1 of the paper (Figure S2).

- TEM micrograph of $LuPO_4$ particles doped with 15% Eu^{3+} obtained in the conditions described in Figure 1 of the paper (Figure S3).

- XRD patterns of $LuPO_4$ nanoparticles doped with different Eu^{3+} contents (Figure S4).

References

1 G. Blasse, B. C. Grabmaier, *Luminescent Materials*. Springer Verlag. Berlin, **1994**.

2 E. L. Cates, S.L. Chinnapongse, J. H. Kim, J.H. Kim, *Environ. Sci. Technol.,* 2012, **45**, 12316-12328.

3 M. Shang, C. Li, J. Lin, *Chem. Soc. Rev.,* 2014, **43**, 1372-1386.

4 D. K. Chatterjee, M. K. Gnanasammandhan, Y. Zhang, *Small,* 2010, **6**, 2781-2795.

5 X. Li, F. Zhang, D. Zhao, *Nano Today,* 2013, **8**, 643-676.

6 L. Zhang, L. Fu, X. Yang, Z. Fu, X. Qi, Z. Wu, *J. Mater. Chem. C,* 2014, **2**, 9149-9158.

7 K. Hickmann, V. John, A. Oertel, K. Koempe, M. Haase, *J. Phys. Chem. C,* 2009, **113**, 4763-4767.

8 Y. Xing, M. Li, S. A. Davis, S. Mann, *J. Phys. Chem. B,* 2006, **110**, 1111-1113.

9 R. X. Yan, X. M. Sun, X. Wang, Q. Peng, Y. D. Li, *Chem. Eur. J.,* 2005, **11**, 2183-2195.

10 A. I. Becerro, S. Rodriguez-Liviano, A. J. Fernandez-Carrion, M. Ocaña, M. *Cryst. Growth & Design,* 2013, **13**, 526-535.

11 W. Ren, G. Tian, L. J. Zhou, W. Y. Yin, L. Yan, S. Jin, Y. Zu, S. J. Li, Z. J. Gu, Y. L. Zhao, *Nanoscale,* 2012, **4**, 3754-3760.

12 S. Rodriguez-Liviano, A. I. Becerro, D. Alcantara, V. Grazú, J. M de la Fuente, M. Ocaña, M. *Inorg. Chem.,* 2013, **52**, 647-654.

13 Y. Li, T. Chen, T.; W. Tan, D. R. Talham, *Langmuir,* 2014, **30**, 5873-5879

14 Y. Gao, M. Fan, Q. Fang, B. Song, W. Jiang, *J. Nanosci. Nanotech.,* 2013, **13**, 6644-6652.

15 S. Heer, O. Lehmann, M. Haase, H. U. Güdel, *Angew. Chem. Int. Ed.,* 2003, **42**, 3179-3182.

16 O. Lehmann, H. Meyssamy, K. Kömpe, H. Schnablegger, M. Haase, *J. Phys. Chem. B,* 2003, **107**, 7449-7453.

17 B. J. Shen, L. D. Sun, J. D. Zhu, L. H. Wei, C. H. Yan *Adv. Func. Mater.,* 2010, **20**, 3708-3714.

18 Y. X. Ni, J. M. Hughes, A. N. Mariano, *Am. Mineral.,* 1995, **80**, 21-26.

19 N. O. Nuñez, M. Ocaña. *Nanotechnology,* 2007, **18**, 455606.

20 N. O. Nuñez, S. R. Liviano, M. Ocaña, *J. Coll. Int. Sci.,* 2010, **349**, 484-491.

21 V. K. Lamer, R. J. Dinegar, *J. Am. Chem. Soc.*, 1950, **72**, 4847-4854.

22 M. Ocaña, M. P. Morales, C. J. Serna, *J. Coll. Int. Sci.* 1995, **171**, 85-91.

23 R. D. Shannon, *Acta Cryst. A*,1976, **32**, 751-767.

24 L. Vegard, *Z. fur Physik,* 1921, **5**, 17-26.

25 R. Yan, Y. Li, *Adv. Funct. Mater.,* 2005*,* ***15***, 763-770.

26 S. Rodriguez-Liviano, F. J. Aparicio, T. C. Rojas, A. B. Hungría, L. E. Chinchilla, M. Ocaña, *Cryst. Growth Des.* 2012*,* **12**, 635−645.

27 P. A. Tanner, *Chem. Soc. Rev*., 2013, **42**, 5090-5101.

28 I. Y. Toth, E. Illes, R. A. Bauer, D. Nesztor, M. Szekeres, Y. Zupko, E. Tomba, *Langmuir,* 2012, **28**, 16638-16646.

29 N. O. Nuñez, S. Rivera, D. Alcantara, J. M. de la Fuente, J. García-Sevillano, M. Ocaña, *Dalton Trans.,* 2013, **42**, 10725-10734.

Table 1: Dimensions of $LuPO_4$ nanoparticles doped with different Eu^{3+} contents. The values have been obtained from counting around a hundred particles of each type in TEM images.

Eu content /%)	Length(sd) (nm)	Width(sd) (nm)
0	130(19)	62(9)
2.5	90(8)	45(5)
5	85(8)	40(5)
10	50(5)	30(3)

Figure captions

Figure 1: SEM and TEM images of $LuPO_4$ nanoparticles synthesized from Lutetium acetate (0.025 M) and H_3PO_4 (0.1 M) in BG solution at 180ºC for 30 minutes.

Figure 2: XRD pattern of the particles shown in Figure 1. The PDF 00-043-0003 (tetragonal $LuPO_4$) is shown on the bottom.

Figure 3: *a)* HRTEM image of a single $LuPO_4$ nanoparticle and intensity profile along the white line showing a regular separation between peaks of 3.5 Å. *b* and *c)* Magnification of the quadrangles shown in *a)* and *b)*, respectively where two families of planes can be observed. The inset is the digital diffraction pattern obtained from the HRTEM image shown in *c)*.

Figure 4: TEM micrographs of three different intermediates in the formation of the $LuPO_4$ nanoparticles. Also shown are the XRD patterns corresponding to such intermediates and PDF 00-043-0003 of tetragonal $LuPO_4$.

Figure 5: TEM micrographs of the Eu^{3+}-doped $LuPO_4$ nanoparticles with different Eu^{3+} contents. The bar size is 200 nm.

Figure 6: Unit cell volume of the Eu^{3+}-doped $LuPO_4$ nanoparticles as a function of Eu^{3+} concentration calculated by the Rietveld analysis of their corresponding XRD patterns. The error bars are of the symbol size.

Figure 7: *Top:* Excitation spectrum of the 5% Eu^{3+}-doped $LuPO_4$ nanoparticles recorded at an emission wavelength of 593 nm. *Bottom:* Emission spectra of different Eu^{3+}-containing $LuPO_4$ nanoparticles recorded at an excitation wavelength of 395 nm.

Figure 8: Integrated area of the emission spectra of the Eu^{3+}-doped $LuPO_4$ nanoparticles as a function of Eu^{3+} concentration. The inset is a CIE diagram showing the chromatic coordinates of the Eu^{3+}-doped particles.

Figure 9: *Top*: FT-IR spectra of the 5% Eu^{3+}-doped $LuPO_4$ particles before and after the functionalization treatment with PAA, and FT-IR spectrum of pure PAA. *Bottom*: Thermogravimetry curves of the 5% Eu^{3+}-doped $LuPO_4$ particles before and after the functionalization treatment with PAA.

Figure 10: Hydrodynamic diameter obtained by DLS measurements for the 5% Eu^{3+}-doped $LuPO_4$ particles functionalized with PAA and dispersed in MES (pH 6.5) and PBS (pH= 7.2) (top and bottom, respectively), after different aging periods at room temperature.

Figure 1

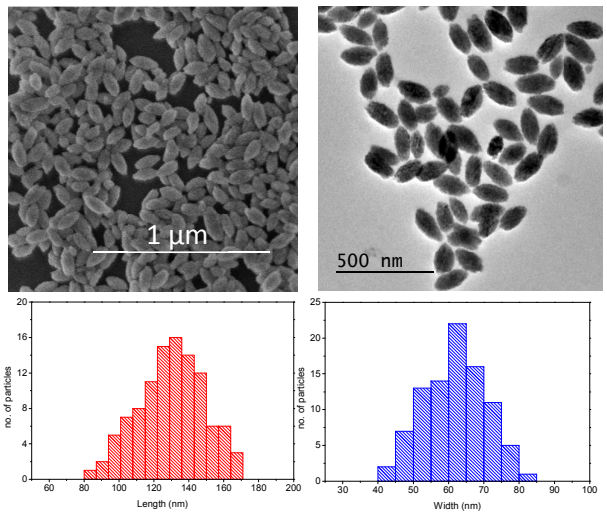

Figure 2

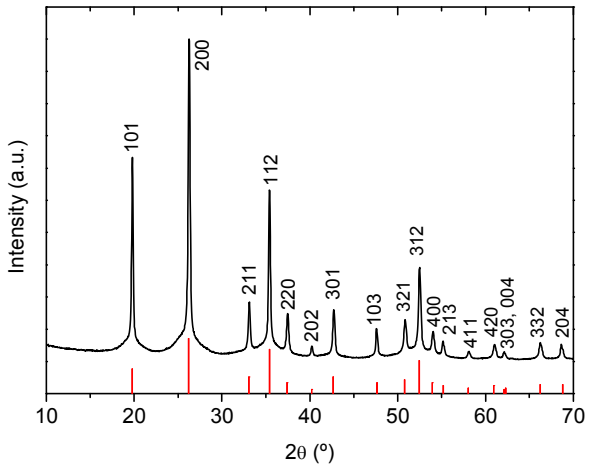

Figure 3

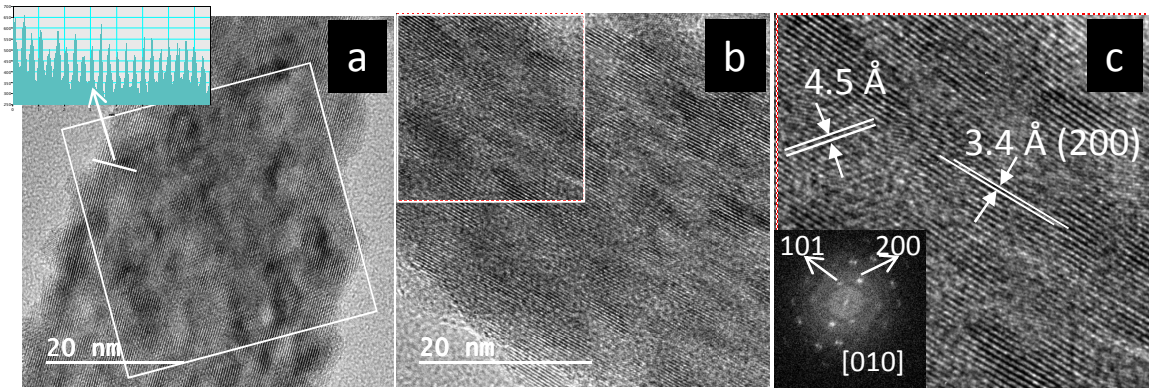

Figure 4

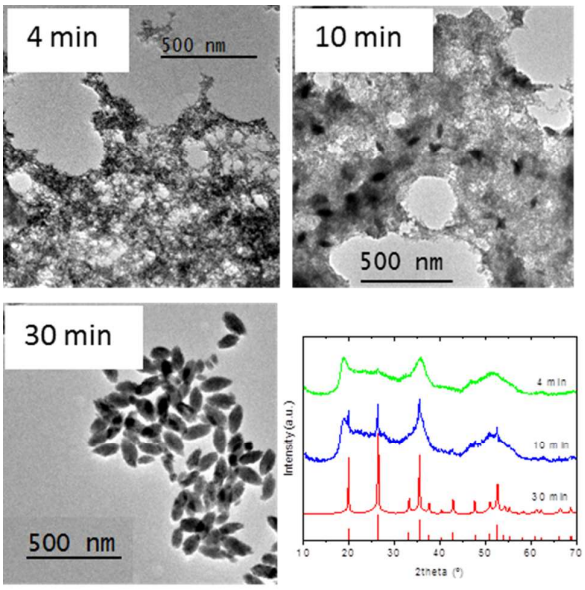

Figure 5

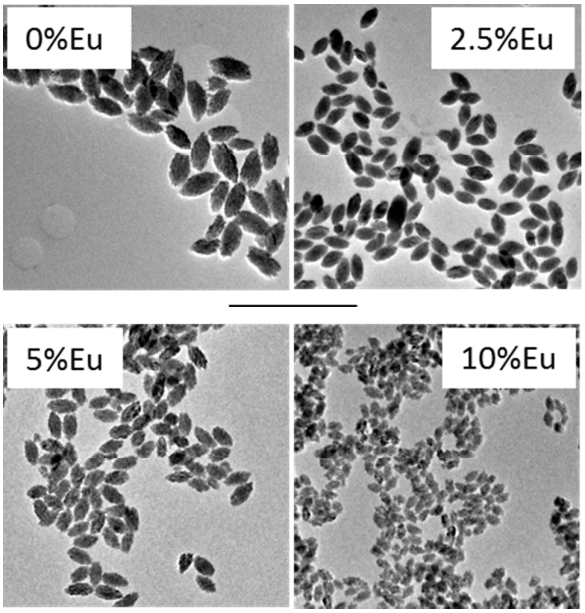

Figure 6

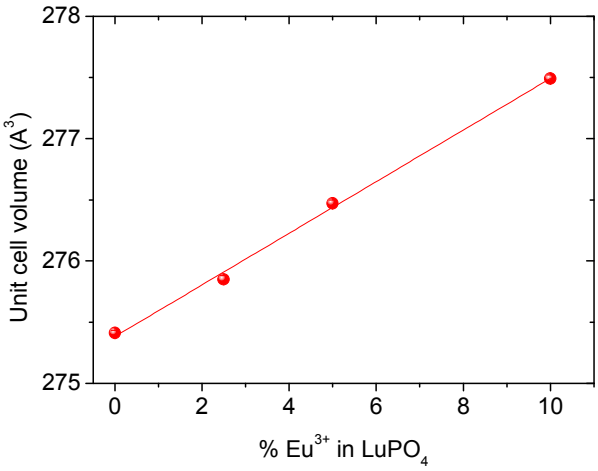

Figure 7

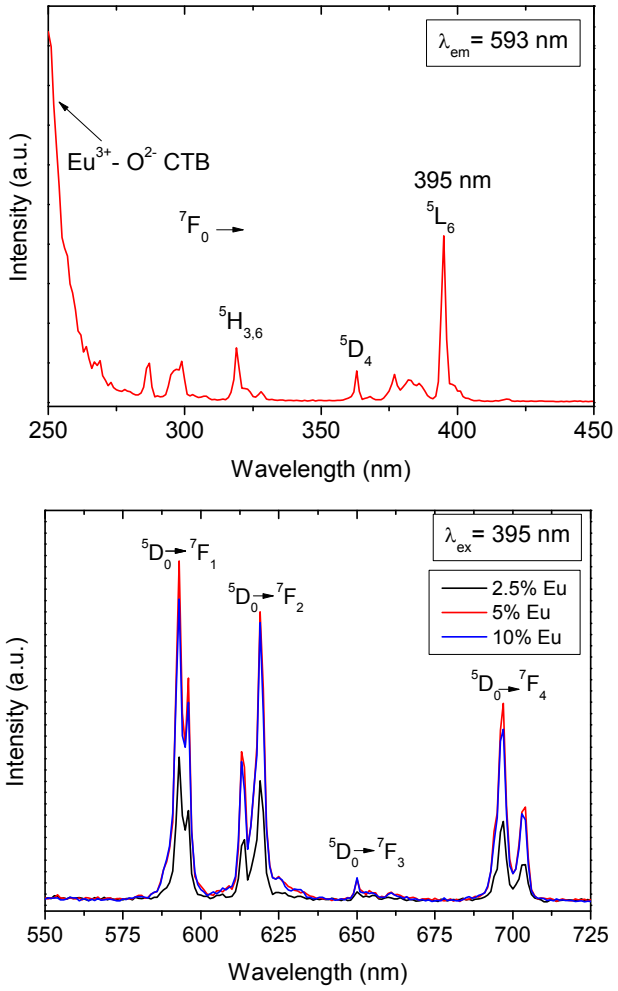

Figure 8

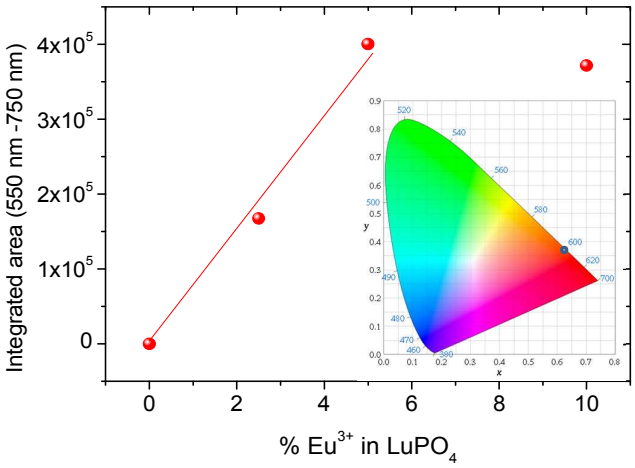

Figure 9

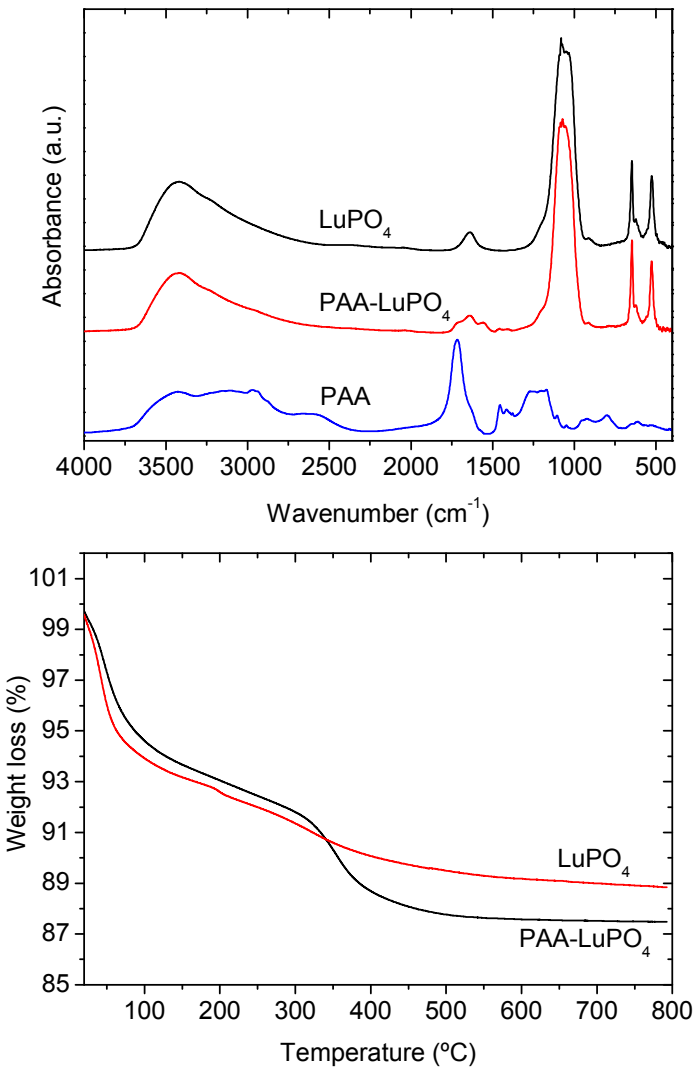

Figure 10

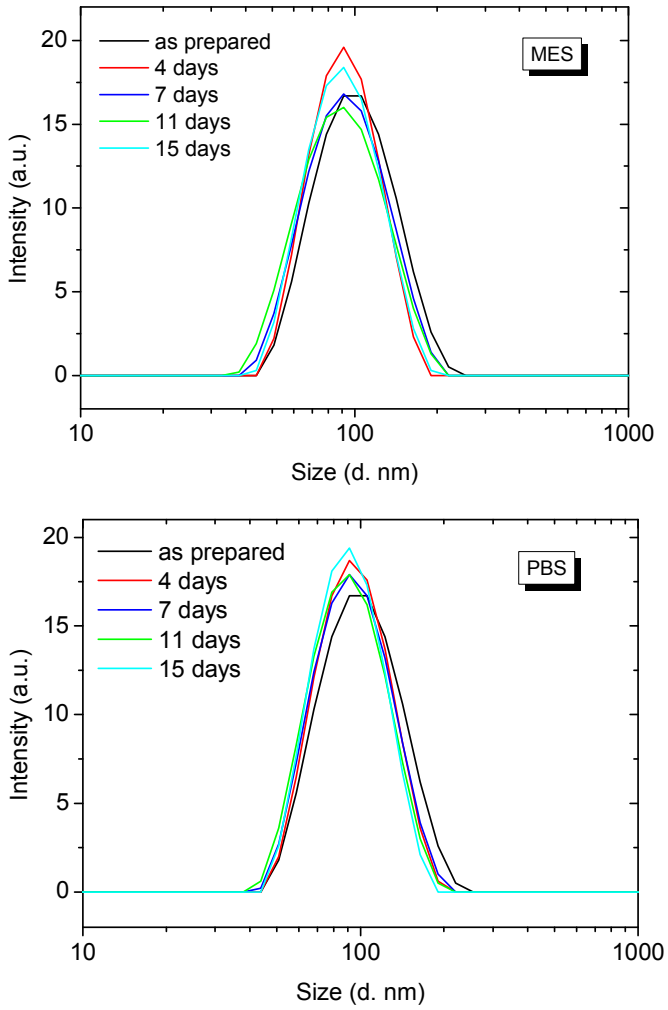

Table of contents

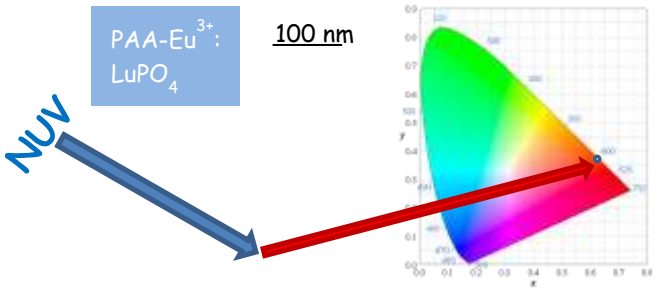

Nanometric, luminescent Eu:$LuPO_4$ particles quickly (30 min) synthesised in the absence of organic additives and able to form stable colloidal suspensions in aqueous media.